

Full Length Research Paper

Polarization synthetic aperture radar (SAR) data for mapping coastal zone vegetation

Maged Marghany*, Noradilawaty Zabidi, Wan Hazli Wan Kadir and Mazlan Hashim

Institute of Geospatial Science and Technology (INSTeG), Universiti Teknologi Malaysia, 81310 UTM, Skudai, Johor Bahru, Malaysia.

Accepted 6 October, 2011

Coastal vegetation is one of the important natural ecosystems that act as protection from sea wave erosion phenomena and supply oxygen to the surrounding organisms. POLSAR data with multi-band and multi-polarization is selected for these studies which are acquired on September 19, 2000, for coastal vegetation mapping. Two methods are performed to C_{VV}, L_{HH} and L_{HV} bands: Polarization signature analysis and comparison of classification between two clustering techniques (Fuzzy-k-mean and iterative self organizing data analysis technique, ISODATA). The result shows that L band with HV polarization can distinguish coastal vegetation better than C_{VV}. Furthermore, classification result of L_{HH} and L_{HV} show that the Fuzzy-k-mean clustering provided accuracy of 76% moreover with the kappa statistic of 70%.

Key words: Polarization synthetic aperture radar (POLSAR), coastal vegetation, polarization signature, fuzzy-k-mean, iterative self organizing data analysis technique (ISODATA).

INTRODUCTION

The main objective of this study is utilizing airborne synthetic aperture radar (AIRSAR)/ polarization synthetic aperture radar (POLSAR) data for mapping coastal vegetation covers. This objective is divided into three objectives: (i) To identify coastal vegetation kinds using AIRSAR/POLSAR, (ii) To determine appropriate polarization band that can distinguish between coastal vegetation types, and (iii) To compare between Fuzzy-k-mean and ISODATA clustering techniques by using error matrix and kappa statistic. Thus it might be to identify the accurate method for coastal vegetation covers mapping.

The vegetations that rise on beaches arises communities recognized as coastal vegetation. Discreet vegetation bands or 'zones' are a widespread feature, reflecting seaside conditions and soil development. Coastal vegetation is itself dynamic. Earlier, simpler vegetation communities pave the way for a series of future, more complex communities. This process is known as succession and is exposed in the formation of

distinct "zones" that run parallel to the shore. Coastal zone vegetations are scattered onshore and offshore. Onshore vegetation covers have an inner landward limit 5 km from coastline while offshore vegetations scattered 200 nautical miles from shoreline (Kennish, 2001). Unfortunately, much of the world coastal vegetation has been modified or cleared for development, leaving us with only "snap shots" of what were once extensive, dynamic and valued vegetation communities (Ande et al., 2009; Akintorinwa and Adesoji, 2009; Josiah and Otieno, 2009; Muhammad et al., 2011; Habibah et al., 2011; Odinga et al., 2011).

Particularly, coastal zone is considered as the most productive ecosystems with reserve biodiversity system (Zelina et al., 2000). In addition, coastal zone vegetation covers play tremendous role in the evaluation of natural management. For instance, they might act as natural defense to protect coastline from erosion impact. However, few studies have been conducted along Malaysian coastal waters to utilize remote sensing data for mapping coastal zone vegetation covers. Furthermore, Mazlan et al. (1999) have used multi temporal JERS-1 SAR data for forest mapping and biomass indicators along the coastal water of Malacca Straits. They reported that the majority of coastal zone spatial forest distributions consist of mangrove with

*Corresponding author. E-mail: maged@utm.my or magedupm@hotmail.com.

Abbreviations: ATI, Along-track interferometric; RSO, rectified skew orthomorphic; SSI, speckle suppression index; PI, polarization indices.



Figure 1. Location of study area.

producer accuracy of 71%. In addition, Mohd et al. (1998) studied the coastal vegetation coverage by using ERS-1 database on spatial variation of radar backscatter. They concluded that the different species existed along coastal zone are consistent with backscatter values acquired from ERS-1 SAR data. Recently, Liali (2002) used segmentation technique for mapping oil palm biomass variation from polarized AIRSAR data. Liali (2002) stated that different polarization bands of AIRSAR data are appropriate to determine certain age of oil palm trees. Band L-hh is able to determine the younger oil palm tree's ages ranged between 6-20 years old. In contrast, oil palm tree's ages have ranged between 21 and 25 can be mapped by using P-hh band. Finally, he concluded that the Gamma algorithm with kernel size of 11×11 is most appropriate to determine the spatial variations of oil palm s' ages. The scope of this study focusing on using AIRSAR/ POLSAR data with C and L band of HH, VV, and HV, respectively to determine the coastal vegetation spatial variations along coastal water of Marang, Terengganu, Malaysia.

STUDY AREA

The study area is located along the east coast of Malaysia which is bordered by the South China Sea. The Marang River is considered is second hydraulic water communication with the South China Sea after Terengganu River. Marang is 20 km from Kuala Terengganu. It is a gateway to the famous Kapas Island and Gemial Island. This area is covered $10 \times 10 \text{ km}^2$ and located between $5^{\circ} 12' 00'' \text{ N}$ and $103^{\circ} 13' 00'' \text{ E}$

(Figure 1). Marang river safari is dominated by mangrove forest and various animal's species that live along the river such birds, lizards, monkeys, crabs etc.

The dominant vegetation species is the forest, bush, various crops, mangrove and paddy. According to Zelina et al. (2000), the mainland mangrove vegetation is both patchy and isolated and often not diverse. Further, Zelina et al. (2000) have stated that the *Nimpa Frutios* is growth extensively along the river banks of Marang and associated with other mangrove species. Moreover, mangrove vegetation exists in patches or in long narrow belt. Finally, the mangrove species do not show clear zonation of individual species distribution.

MATERIALS AND METHODS

Figure 2 illustrates the flow chart of AIRSAR/POLSAR data processing for mapping vegetation species. The main image processing is divided into data enhancement and data classification. Data classification is done using fuzzy-k-mean and ISODATA clustering techniques.

Data acquisition

The Jet Propulsion Laboratory (JPL) airborne synthetic aperture radar (AIRSAR/POLSAR) data AIRSAR/POLSAR is a NASA/JPL multi-frequency instrument package aboard, a DC-8 aircraft and operated by NASA's Ames Research Center at Moffett Field. AIRSAR flies at 8 km over the average terrain height at a velocity of 215 ms^{-1} . The system is designed to be flown on small and large aircraft. The system requires a scanner port ($18 \text{ cm} \times 36 \text{ cm}$) on the aircraft underside. JPL's airborne synthetic aperture radar (AIRSAR/POLSAR) is a unique system, comprising of three radars at HH-, VV-, HV- and VH-polarized signals from $5 \text{ m} \times 5 \text{ m}$ pixels

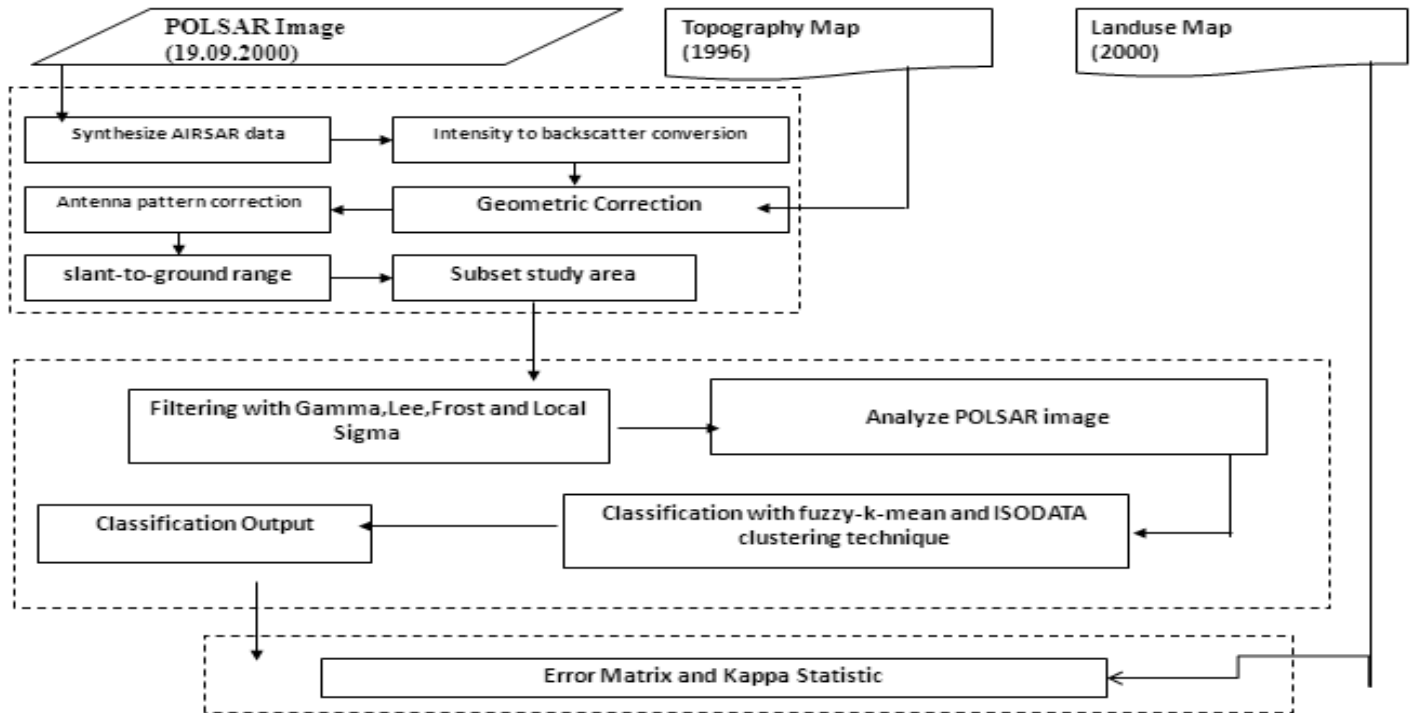


Figure 2. Flow chart of AIRSAR/POLSAR data processing for vegetation's species mapping.

recorded for three wavelengths: C band (5 cm), L band (24 cm) and P band (68 cm) (Zebker, 1992). AIRSAR data collections involved; fully polarimetric data (POLSAR) can be collected at all three frequencies, while cross-track interferometric data (TOPSAR) and along-track interferometric (ATI) data can be collected at C- and L-bands (Marghany and Mazlan, 2011).

Pre-image processing

Synthesize POLSAR data

POLSAR images are in compressed format. Images of the POLSAR data must be mathematically synthesized or decompress from the compressed scattering matrix data accordingly, before usage in the next processing. The input POLSAR must be in JPL stokes matrix format.

Geometric correction

The process of geometric correction must be carried out to match the image according to RSO (Rectified Skew Orthomorphic) projection. The geometric correction is done from map to image. There are 25 ground control points that have been identified, and digital number is transformed using second degree polynomial order and lastly image is resampled using Nearest Neighbour technique (Lillesand and Kiefer, 2000).

Antenna signature correction

An inherent problem with airborne radar data owing to the side-looking nature of the system is an increased brightness or gain in

energy of the signal in the near-range than far-range. Therefore, it must be corrected using first order polynomial without removing the local variation in backscatter signals (Marghany and Mazlan, 2011).

Slant-to-ground range

According to Mougin et al. (1999) and Marghany and Mazlan (2011), polarized AIRSAR/POLSAR data are required to be converted from ground range to slant range. In fact, slant range radar data has geometric distortion in the range direction. The true or ground range pixel sizes vary across the range direction because of the changing incidence angles. This geometric distortion is corrected by resampling the slant range data to create ground range pixels that are in fixed size. After resampling, the compacted part of the images must be stretched to the correct ground range.

POST-PROCESSING IMAGE

Filtering

Image enhancement is used to visualize unclear features (El-Sayed, 2007; Nishat and Elwin, 2009). Spatial filtering is a necessary and effective method to suppress the "salt and pepper" effects of speckle in the radar brightness data (Marghany and Mazlan, 2010). Three types of adaptive filter algorithms are tested: (i) Lee, (ii) Gamma, and (iii) Frost. These algorithms are implemented to AIRSAR/POLSAR image with kernel window sizes of 3×3 , 5×5 and 7×7 pixels and lines. The SSI (speckle suppression index) and differentiation statistic values used to identify an appropriate algorithm. In this context, the suitable adaptive algorithm should reduce SSI value to be close to 1. In addition, the lower standard deviation value might be a good

Table 1. Parameters in FUZCLUS and ISOCLUS.

Parameter	Technique	
	FUZCLUS	ISOCLUS
Number of cluster desired	30	30
Maximum number of clusters	-	35
Minimum number of cluster	-	20
Standard deviation	-	10
Lumping parameter	-	1
Maksimum number of lumping	-	5
Pairs	0.5	0.5
Movement threshold	20	20
Maximum number of iteration	-	-

indicator for suitable adaptive algorithm.

Classification using clustering technique

Consistent with Mouing et al. (1999) and Khadijeh et al. (2011), clustering technique operates using two spectral bands to provide band correlation. Prior to clustering process, the band configuration should determine. From spread out scattering matrix Muller (Equation 1), the co and cross-polarize have difference backscatter. In this regards, correlation between both polarized bands is obtained. Consequently, the AIRSAR/POLSAR data have four polarization bands of C-HH and C-VV, C-HV, L-HH and L-VV, and L-HV (Liali, 2002).

$$\begin{matrix} U_v^r \\ U_h^r \end{matrix} = \begin{matrix} S_{vv} S_{vh} \\ S_{hv} S_{hh} \end{matrix} \begin{matrix} U_v^t \\ U_h^t \end{matrix} \quad 1$$

Clustering is the processes to examine the unknown pixels in an image and aggregate them into a number of classes based on the natural groupings or clusters present in the image value. Two clustering techniques are examined on AIRSAR/POLSAR data. Fuzzy-k-mean and ISODATA algorithms are implemented to airborne polarized data. In doing so, several parameters for instance, the number of cluster desired, maximum number of clusters, minimum number of cluster, standard deviation, etc are set up as shown in Table 1 for both algorithms.

Additionally, polarization indices (PI) analysis is performed to determine spatial distribution of polarization indices for coastal vegetation in co-polarize (HH and VV) and cross-polarize (HV). According to Proisy et al. (2001), PI is the ratio between the sums and subtracts from the minimum, and maximum polarization intensity value which has been described by Touzi et al. (1992) and Touzi (2002) by following formula:

$$PI = (P_{\max} - P_{\min}) / (P_{\max} + P_{\min}) \quad 2$$

where P_{\max} and P_{\min} are the maximum and minimum values of polarization intensity.

Accuracy assessment

To identify the accuracy of the techniques implemented to AIRSAR/POLSAR data, error matrix and the Kappa statistic are used. In this context, the appropriate technique might have the

highest accuracy which would be useful to determine coastal vegetation species.

RESULTS AND DISCUSSION

Figure 3 shows the output results of Gamma algorithm with kernel size of 7×7 . It is clear that speckle variations are reduced after performing Gamma algorithm (Figure 3b). This result is agreed with Figure 4 which shows that Gamma algorithm produce image with a lower SSI value of 0.84 within C-HH band compared to L-HH band. According to Marghany and Shattri (1996) and Marghany (2001) Gamma algorithm mapped homogenous regions and provides a classified land covers (Figure 3a). Thus, Gamma algorithm provides very high speckle reduction, while preserving the spatial resolution (Marghany, 2001).

Figure 5 shows that band L-cross polarization has higher PI values for various vegetation species than band C (cross-polarization and co-polarization). In fact, PI discriminates between coastal vegetation classes. In addition, the polarization signature method shows that L band with hv polarization is able to discriminate between various species of coastal vegetation. According to Proisy et al. (2001), L-HV band can penetrate from canopy level to land surface compared to C band (Mougin et al., 1999). In addition, HV polarization signal is transmitted in horizontal (H) and received in vertical (V) which allowed capturing complete characteristics of vegetation covers (Rao and Gurusamy, 1990; Proisy et al., 2000; Guihong and Peter, 2003).

Figure 6 shows the variation of vegetation species produced by using Fuzzy-k-mean and ISODATA clustering techniques. Fuzzy-k-mean clustering has higher accuracy value of 76% than ISODATA clustering accuracy value of 67% as shown in Table 2. This could be contributed to that Fuzzy-k mean clustering provides continuous classes and better representations of outliers or atypical individuals than discontinuous classes (Liew et al., 2000). Figure 7 shows the percentage variation of vegetation species along the coastal water of Terengganu, Malaysia. It is obvious that dominant

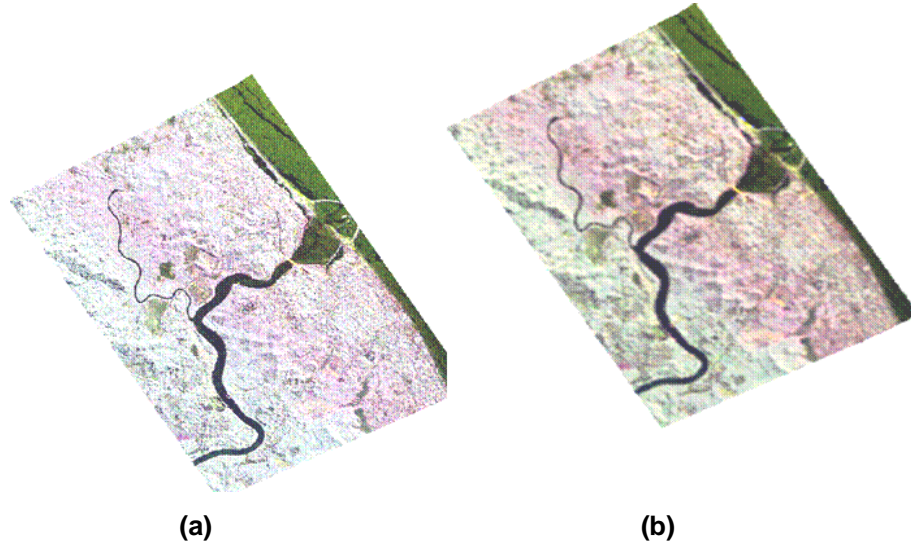


Figure 3. AIRSAR/POLSAR image; (a) without filter (b) with Gamma 7x7.

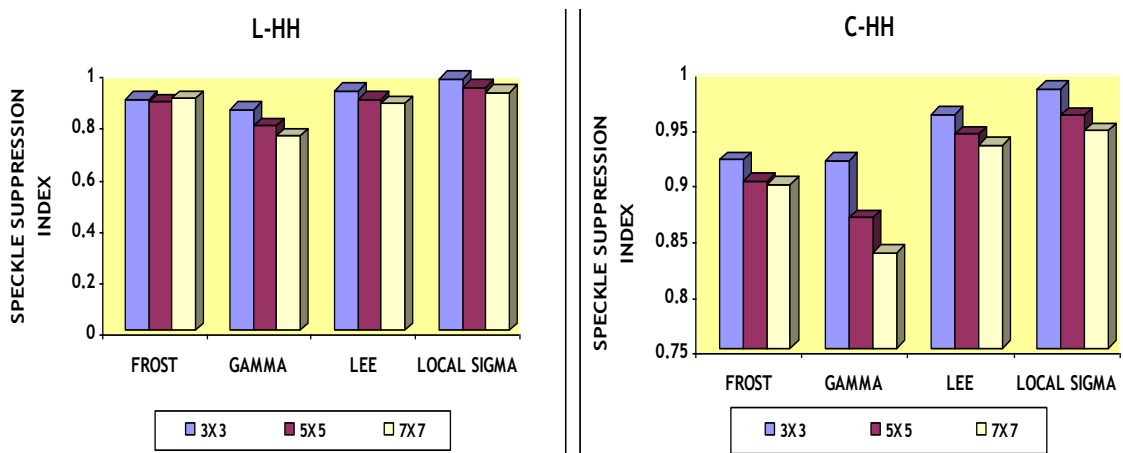


Figure 4. SSI values for each Adaptive Algorithm tested in C-hh and L-hh Bands.

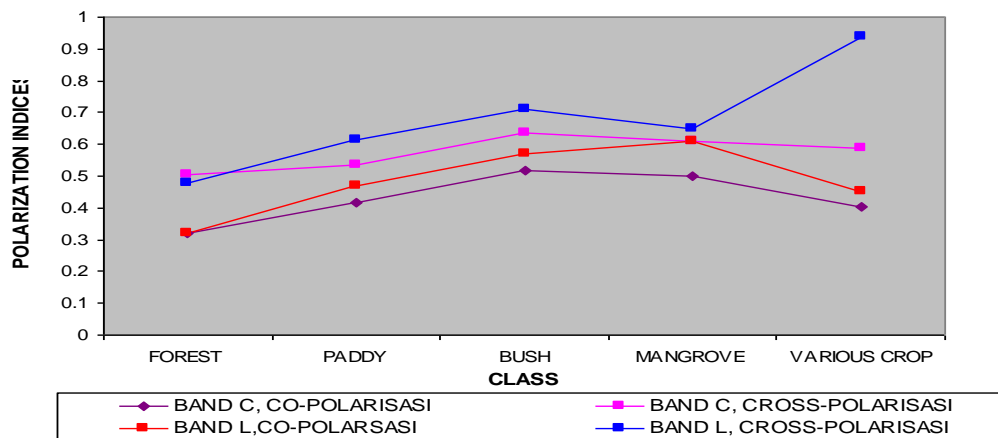


Figure 5. Polarization indices for C and L bands.

CLASSIFICATION MAP FOR COASTAL VEGETATION IN MARANG, TERENGGANU

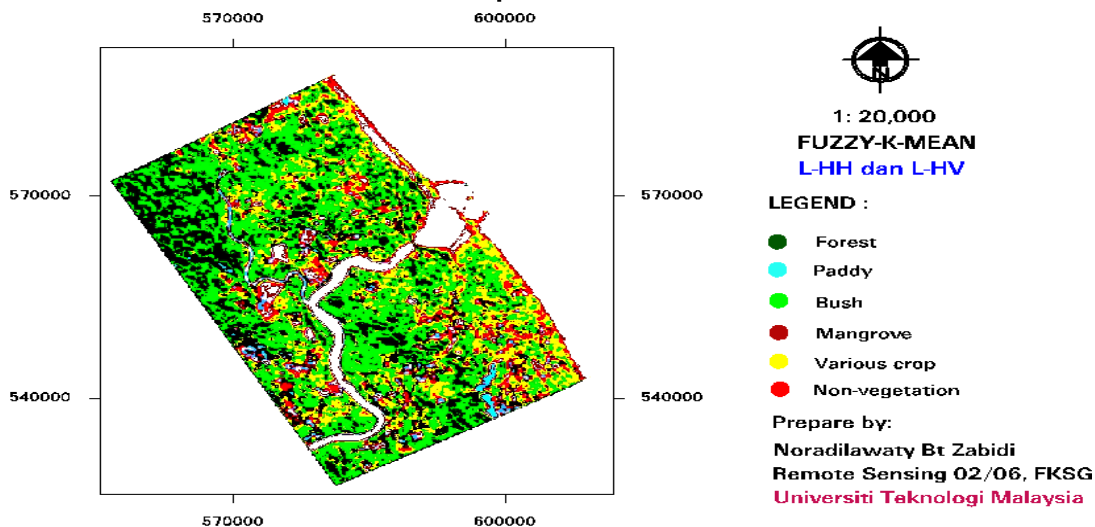


Figure 6. Classification map of L-HH and L-HV configuration using fuzzy-k-mean algorithm.

Table 2. Accuracy Assessments of Fuzzy-k-mean and ISODATA.

Classification technique	Configuration	Overall accuracy (%)	Kappa statistic (%)
Fuzzy-k-mean	C-HH and C-VV	58	51
	C-HH and C-HV	63	55
	L-HH and L-VV	52	48
	L-HH and L-HV	76	70
ISODATA	C-HH and C-VV	48	40
	C-HH and C-HV	53	45
	L-HH and L-VV	56	53
	L-HH and L-HV	67	59

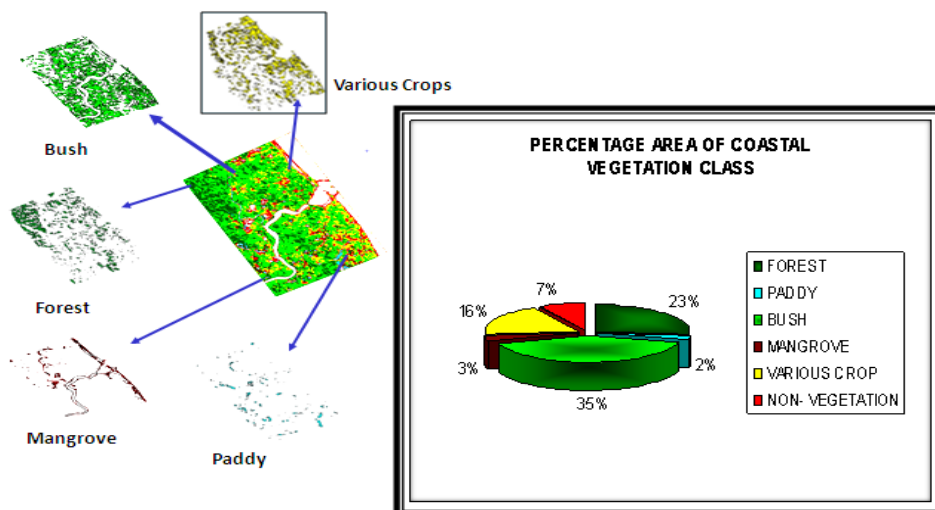


Figure 7. Percentage of coastal vegetation species.

vegetation species is the bush with 35% which covers 810.11 ha compared to paddy, forest, mangrove, various crops and non-vegetation with 2% (50.90 ha), 23% (539.2 ha), 3% (52.90 ha), 16% (375.14 ha) and 7% (169.84 ha) respectively as shown in Figure 7.

Conclusion

This work has presented method to map vegetation species types that are grown along the east coast of Peninsular Malaysia. The image clustering methods of Fuzzy-k-mean and ISODATA implemented to AIRSAR/POLSAR polarized data. The study shows that the gamma algorithm with kernel size 7×7 is more appropriate for speckle noise reductions which provide lower SSI value of 0.84 compared to other adaptive algorithm. In addition, fuzzy-k-mean algorithm shows excellent performance for vegetation covers mapping compared to ISODATA algorithm. Overall accuracy of fuzzy-k-mean is 76% which is higher than ISODATA algorithm accuracy. Besides, the main coastal vegetation species that existed along coastal waters are forest, paddy, bush, mangrove and various crops. In these regards, the main dominated vegetation species is the bushy. In conclusion, L-HV polarization is suitable band for mapping various vegetation species by using AIRSAR/POLSAR data.

REFERENCES

- Akintorinwa OJ, Adesoji JI (2009). Application of geophysical and geotechnical investigations in engineering site evaluation. *Int. J. Phys. Sci.*, 4(8): 443-454.
- Ande OT, Alaga Y, Oluwatosin GA (2009). Soil erosion prediction using MMF model on highly dissected hilly terrain of Ekiti environs in southwestern Nigeria. *Int. J. Phys. Sci.*, 4(2): 053-057.
- El-Sayed WM (2007). Image enhancement using second generation wavelet super resolution. *Int. J. Phys. Sci.*, 2(6): 149-158.
- Guihong C, Peter B (2003). Fuzzy K-means clustering in information retrieval. *IEEE Trans. Geosci. Remote Sensing*, 22: 198-200.
- Liali N (2002). Application of AIRSAR Data to Oil Palm tree Characterization. www.gisdevelopment.net/aars/acrs/2002/sar/038.pdf.
- Liew AW, Leung SH, dan Lau WH (2000). "Fuzzy Image Clustering Incorporating Spatial Continuity." *IEEE Trans. Geosci. Remote Sensing*, 147(2): 185-192.
- Lillesand TM, Kiefer RW (2000). Remote sensing and image interpretation. 4th Ed. Wiley, USA, NewYork.
- Josiah A, Otieno F (2009). Optimizing planting areas using differential evolution (DE) and linear programming (LP). *Int. J. Phys. Sci.*, 4(4): 212-220.
- Habibah L, Abu BM, Khan YA, Abustan I (2011). Influence of tensile force of agave and tea plants roots on experimental prototype slopes. *Int. J. Phys. Sci.*, 6(18): 4435-4440.
- Khadijeh M, Motameni H, Enayatifar R (2011). New method for edge detection and de noising via fuzzy cellular automata. *Int. J. Phys. Sci.*, 6(13): 3175-3180.
- Kennish MJ (2001). Coastal salt marsh systems in the U.S.: A review of anthropogenic impacts. *J. Coastal Res.*, 17: 731-748.
- Marghany M (2001). Radar Automatic Detection Algorithms for Coastal Oil Spills Pollution. *Int. J. Appl. Earth Observation Geo-inform.*, 3(2): 191-196.
- Marghany M, Shattri M (1996). On the application of Radarsoft to Extract Infrastructure Details from RADARSAT. Proceedings of Seminar Malaysian Remote Sensing Society Conference on Remote Sensing and GIS 25-27 November 1996. Crown Prince Hotel, Kuala Lumpur. C1-C6.
- Marghany M, Mazlan H (2011). Discrimination between oil spill and look-alike using fractal dimension algorithm from RADARSAT-1 SAR and AIRSAR/POLSAR data. *Int. J. Phys. Sci.*, 6(7): 1711-1719.
- Marghany M, Mazlan H (2010). Developing adaptive algorithm for automatic detection of geological linear features using RADARSAT-1 SAR data. *Int. J. Phys. Sci.*, 5(14): 2223-2229.
- Muhammad M, Baidillah MR, Taha MR, El-Shafie A (2011). Effect of soil water retention model on slope stability analysis. *Int. J. Phys. Sci.*, 6(19): 4629-4635.
- Mazlan H, Hazli W, Kadir W, Yoong LK (1999). Global Rain Forest Mapping Activities in Malaysia: Radar Remote Sensing for Forest Survey and Biomass indicators. JERS-1 Science Program '99 PI Reports: Global Forest Monitoring and SAR Interferogram March 1999, earth Observation Reserch Centre. National space development Agency of Japan, pp. 63-70.
- Mohd IS, Samsudin A, Adeli A (1998). Investigation of ERS-1 SAR and LANDSAT TM for land and marione applications in Malaysia. Proceedings of the Euro-Asia space, Week on Cooperation in Space- 'Where east&west Finally Meet', 23-27 November 1998, Singapore (ESA SP-430, February 1999), pp. 67-74.
- Mougin E, Proisy C, Marty G, Fromard F, Puig H, Betouille JL, Rudant JP (1999). Multifrequency and multipolarization radar backscattering from mangrove forests. *IEEE Trans. Geosci. Remote Sensing*, 37(1): 94-102.
- Nishat K, Elwin CM (2009). Adaptive lifting based image compression scheme for narrow band transmission system. *Int. J. Phys. Sci.*, 4(4): 194-164.
- Odinga C, Otieno F, Adeyemo J (2011). Investigating the effectiveness of aquatic plants (Echinocloa L and Cyperus L) in removing nutrients from wastewater: The case of Chemelil constructed wetland-Kenya. *Int. J. Phys. Sci.*, 6(16): 3958-3968.
- Proisy C, Mougin E, Fromard F, Karam MA (2000). Interpretation of polarimetric radar signatures of mangrove forests. *Remote sensing Environ.*, 71: 56-66.
- Proisy C, Mougin E, Fromard F (2001). Radar remote sensing of mangroves: results and perspectives. Proceedings of IGARSS Conference (9-13 July), Sydney, Australia, 7: 3056-3058.
- Rao KS, Gurusamy R (1990). Frequency dependence of polarization phase difference and Polarization indices for vegetation covered fields using polarimetric AIRSAR Data". *IEEE Trans. Geosci. Remote Sensing*, 1(1): 37-39.
- Touzi R, Gozs S, Toan TL (1992). "Polarimetric Discriminators for SAR Images." *IEEE Trans. Geosci. Remote Sensing*, 30(5): 973-980.
- Touzi R (2002). A review of speckle filtering in the context of estimation theory. *IEEE Trans. Geosci. Remote Sensing*, 40: 2392-2404.
- Zebker HA (1992). The TOPSAR interferometric radar topographic mapping instrument. *IEEE Trans. Geosci. Remote Sensing*, 30: 933-940.
- Zelina ZI, Arshad A, Lee SC, Japar S, Law AT, Nik MRA, Maged MM (2000). East Coast of Peninsular Malaysia. Sea at the Millennium: an Environmental Evaluation. *In (Ed) Charels Sheppard. Oxford, Il: 345-359.*